Perovskite-type oxide $ACo_{0.8}Bi_{0.2}O_{2.87}$ (A = $La_{0.8}Ba_{0.2}$): a catalyst for low-temperature CO oxidation

H.X. Dai [a,b], H. He [a,c], W. Li [c], Z.Z. Gao [b] and C.T. Au [a,*]

[a] *Department of Chemistry, Hong Kong Baptist University, Kowloon Tong, Hong Kong*
E-mail: pctau@hkbu.edu.hk
[b] *Department of Applied Chemistry, Faculty of Science, Beijing University of Chemical Technology, Beijing 100029, PR China*
[c] *College of Environmental and Energy Engineering, Beijing Polytechnic University, Beijing 100022, PR China*

Received 14 November 2000; accepted 5 March 2001

Perovskite-type oxide $ACo_{0.8}Bi_{0.2}O_{2.87}$ (A = $La_{0.8}Ba_{0.2}$) has been investigated as a catalyst for the oxidation of carbon monoxide. X-ray diffraction results revealed that the catalyst is single-phase and cubic in structure. The results of chemical analysis indicated that in $ACo_{0.8}Bi_{0.2}O_{2.87}$, bismuth is pentavalent whereas cobalt is trivalent as well as bivalent; in $La_{0.8}Ba_{0.2}CoO_{2.94}$, cobalt ions exist as Co^{3+} and Co^{4+}. The substitution of Bi for Co enhanced the catalytic activity of the perovskite-type oxide significantly. Over the Bi-incorporated catalyst, at equal space velocities and with the rise in CO/O_2 molar ratio, the temperature for 100% CO conversion shifted to a higher range; at a typical space velocity of 30000 h^{-1} and a CO/O_2 molar ratio of 0.67/1.00, 100% CO conversion was observed at 250 °C. Over $ACo_{0.8}Bi_{0.2}O_{2.87}$, at equal CO/O_2 molar ratio, the temperature for 100% CO conversion decreased with a drop in space velocity; the lowest being 190 °C at a space velocity of 5000 h^{-1}. The result of O_2-TPD study illustrated that the presence of Bi ions caused the lattice oxygen of $La_{0.8}Ba_{0.2}CoO_{3-\delta}$ to desorb at a lower temperature. The results of TPR, $^{18}O/^{16}O$ isotopic exchange, and CO-pulsing investigations demonstrated that the lattice oxygen of the Bi-doped catalyst is highly mobile.

KEY WORDS: perovskite-type oxide catalyst; $La_{0.8}Ba_{0.2}Co_{0.8}Bi_{0.2}O_{2.87}$; low-temperature CO oxidation; $^{18}O/^{16}O$ isotopic exchange; lattice oxygen mobility; oxidative nonstoichiometry

1. Introduction

Perovskite-type oxides (ABO_3), with the A site being a rare earth metal coordinated by twelve oxygen atoms and located at the cavities in the BO_6 octahedra and the B site being a transition metal surrounded by six oxygen atoms in octahedral coordination, have been investigated extensively and intensively for their physical and catalytic properties. The partial substitution of A and/or B by aliovalent metal ions brings about (i) a change in the oxidation state of B and (ii) structural defects (such as anionic and cationic vacancies) which are generally associated with the physicochemical behaviors of the material [1–3]. Among the perovskites reported in the literature, La-based cobaltates and manganates appear to be the best-performing for the total oxidation of CO and HC (hydrocarbons). Perovskites with both oxidative nonstoichiometry ($\delta < 0$), such as $LaMnO_{3-\delta}$ [4], $LaMn_{1-x}Cu_xO_{3-\delta}$ [5–7], and $La_{1-x}A'_xMnO_{3-\delta}$ (A′ = Ca and Sr) [8], and reductive nonstoichiometry ($\delta > 0$), such as $LaCo_{1-x}Cu_xO_{3-\delta}$ [6], $LaCoO_{3-\delta}$ [9], and $La_{1-x}Sr_xMO_{3-\delta}$ (M = Mn, Co, Cr, Fe) [10–13], have been reported to be catalytically active for the complete oxidation of CO, HC, and/or NH_3. Recently, Ramesh and Hegde [14] claimed that a Co- and Cu-based triple-layered rare earth perovskite, $LaBa_2Cu_2CoO_{7+\delta}$, exhibited high CO conversion to CO_2 at ca. 200 °C; they attributed that to (i) changes in coordination polyhedra around Cu, (ii) promoted oxygen mobility, and (iii) redox potentials of the different transition metal cations. More recently, a pyrochlor-type oxide $Sm_2Cu_{2/3}Nb_{4/3}O_7$ catalyst, with 100% CO conversion under conditions of temperature ca. 300 °C, CO/O_2 molar ratio 2.1/1.0, and space velocity 8000 h^{-1}, has been reported and the authors argued that the good activity could be associated with the oxygen-deficient structure and the variable oxidation states of Cu and Nb [15].

In our previous works, we have characterized and reported a series of $La_{1-x}Sr_xCo_{1-y}M_yO_{3-\delta}$ (M = Cu, V, Sn, Ti, Zr) [16,17] catalysts and found that most of them showed good activities for CO oxidation in the range of 300–400 °C and at 20000 h^{-1}. It has been generally believed that the concentration of adsorbed oxygen species and the mobility of lattice oxygen in perovskites are important factors in the catalytic oxidation of CO. The Sr- or Ba-doped cobaltates $La_{1-x}A'_xCoO_{3-\delta}$ (A' = Sr, Ba) show large oxygen deficiency [18–21]. Bismuth oxides are typical donors of mobile oxygen species [22]. Bismuth is an important component in catalytic materials such as $KBiO_3$ [3], $BaBiO_3$ [23], $BaPb_{1-y}Bi_yO_{3-\delta}$ [24], $KSr_2Bi_3O_4Cl_6$ [25], and Bi_2O_3–SnO_2 [26] as well as in superconducting materials such as $Ba_{1-x}K_xBiO_{3-\delta}$ [27–30] and Bi–Sr–Ca–Cu–O [31–33]. By incorporating a small amount of Bi into the B site of $La_{1-x}A'_xCoO_{3-\delta}$ (A′ = Sr, Ba), we generated several classes of perovskite-type oxide catalysts active for CO oxidation at low temperatures. In this paper, we report the catalytic performance of $ACo_{0.8}Bi_{0.2}O_{2.87}$

---

[*] To whom correspondence should be addressed.

(A = $La_{0.8}Ba_{0.2}$) with oxidative nonstoichiometry and characterized this material by means of techniques such as X-ray diffraction (XRD), temperature-programmed reduction (TPR), temperature-programmed desorption (TPD), and $^{18}O_2$- and CO-pulsing as well as chemical analysis for the oxidation states of cobalt and bismuth.

2. Experimental

The catalysts were prepared by adopting the method of citric acid complexing [4]: (i) $La(NO_3)_3{\cdot}6H_2O$ (Acros, >99%), $Ba(NO_3)_2$ (Aldrich, >99%), $Co(NO_3)_2{\cdot}6H_2O$ (Acros, >99%) (for $La_{0.8}Ba_{0.2}CoO_{3-\delta}$) and (ii) $La(NO_3)_3{\cdot}6H_2O$, $Ba(NO_3)_2$, $Co(NO_3)_2{\cdot}6H_2O$, and $Bi(NO_3)_3{\cdot}5H_2O$ (Aldrich, >98%) (for $ACo_{0.8}Bi_{0.2}O_{3-\delta}$) at the appropriate ratio were mixed in aqueous solution. Citric acid (Aldrich, >99%) equimolar to the metals was added. The solution was then evaporated at 70 °C to produce a viscous syrup. After subsequent evaporation at 120 °C for 8 h and calcination at 850 °C in air for 18 h, the material was in turn ground, tabletted, crushed, and sieved to a size range of 80–100 mesh.

Catalytic activity measurements were carried out at atmospheric pressure with 0.2 ml of the catalyst in a fixed-bed quartz microreactor (i.d. = 4 mm). The total flow rate of the reactant mixture, (i) 1.75% CO + 2.60% O_2 + 95.65% He, (ii) 1.75% CO + 1.00% O_2 + 97.25% He, and (iii) 1.75% CO + 0.87% O_2 + 97.38% He, was 100 $ml\,min^{-1}$; the corresponding CO/O_2 molar ratio was 0.67/1.00, 1.75/1.00, and 2.01/1.00, respectively, and the space velocity was 30000 h^{-1}. The inlet and outlet CO concentrations were analyzed on-line by a nondispersive infrared CO/HC gas analyzer (MEXA-324F, Horiba). For the variation of space velocity, we changed the mass of the catalyst at a fixed flow rate of 100 $ml\,min^{-1}$.

The crystal structure of the catalyst was determined by an X-ray diffractometer (D-MAX, Rigaku) operating at 40 kV and 200 mA using Cu K_α radiation. The patterns recorded were referred to the powder diffraction files – 1998 ICDD PDF database for identification. The specific surface area of the catalyst was measured using the BET method on a Nova 1200 apparatus.

The TPR and O_2-TPD experiments were performed according to the methods described previously [34]. The temperature range was from room temperature to 900 °C and the heating rate was 10 $°C\,min^{-1}$. The amount of O_2 desorbed from the catalyst was quantified by calibrating the peak areas against that of a standard O_2 pulse.

Pulse experiments were performed to investigate the reactivity of oxygen species. A catalyst sample (0.3 g) was placed in a microreactor and was thermally treated in He (HKO, >99.995%, 20 $ml\,min^{-1}$) at a desired temperature for 30 min. We pulsed $^{18}O_2$ (HKO, 95–98%) onto the sample (He as carrier gas, 20 $ml\,min^{-1}$) at various temperatures and monitored the composition of the outlet by means of a mass spectrometer. The data were taken at the 10th pulse where the reaction reached a steady state. In the CO-pulsing experiments, the sample which had in turn been treated in He at 700 °C for 30 min and exposed to 100 pulses of $^{18}O_2$ at 500 °C was exposed to CO pulses (He as carrier gas, 80 $ml\,min^{-1}$) at different temperatures and the effluent was analyzed on-line by a mass spectrometer. The pulse size was 50.0 μl (at 25 °C, 1 atm).

Oku et al. [35] reported a method that could make a distinction between the oxidation states of Cu^{3+} and Bi^{5+} in Bi-based cuprate superconductors. The approach was adopted for the analysis of the oxidation states of Co^{3+} and Bi^{5+} ions in the catalyst. Bi^{5+} can oxidize Mn^{2+} to MnO_4^- (see equation (1)) whereas Co^{3+} is not an oxidizing agent strong enough to accomplish such a task.

$$5Bi^{5+} + 2Mn^{2+} + 14H^+ \rightarrow 5Bi^{3+} + 2MnO_4^- + 7H_2O \tag{1}$$

In the analysis, the sample (ca. 0.1 g) was (i) dissolved in 10 ml of a solution containing 0.25 M $Mn(NO_3)_2$ in 3 M HNO_3, (ii) cooled to room temperature (since the reaction is exothermic) and diluted with 70 ml of cold water, and (iii) treated with 10 ml of standard 0.1 M Fe^{2+} in 1 M H_2SO_4. The MnO_4^- produced in reaction (1) oxidized Fe^{2+} to Fe^{3+}. A mixture of concentrated acids (1.5 ml H_2SO_4 + 1.5 ml H_3PO_4 + 7.0 ml H_2O) was then added and the unreacted Fe^{2+} was titrated against standard 0.017 M $K_2Cr_2O_7$ using sodium 4-diphenylamine sulfonate as the indicator. By so doing, one can obtain the Bi^{5+} content in the sample. In order to find out the total content of Co^{3+} and Bi^{5+}, the sample was dissolved in the acid-containing standard Fe^{2+} solution and the unreacted Fe^{2+} was determined by $K_2Cr_2O_7$ titration; the Fe^{2+} consumed by the sample was equivalent to the total amount of Co^{3+} and Bi^{5+}. By subtracting the Bi^{5+} content, one can obtain the Co^{3+} content in the sample. For the $La_{0.8}Ba_{0.2}CoO_{3-\delta}$ sample, the Co^{3+} content was determined by the iodometric titration method. The experimental errors of the approaches were estimated to be ±0.5%.

3. Results

3.1. Crystal structures, surface areas, and catalytic activities

Figure 1 shows the XRD results of the fresh $La_{0.8}Ba_{0.2}CoO_{3-\delta}$ as well as the fresh and used (after the CO oxidation reaction) $ACo_{0.8}Bi_{0.2}O_{3-\delta}$ catalysts; the patterns obtained after reduction and reoxidation are also included. By comparing the XRD patterns with the ICDD PDF database data of $LaCoO_3$ (No. 7-0279) and $La_{0.5}Ba_{0.5}CoO_3$ (No. 32-0480), one can realize that the fresh $La_{0.8}Ba_{0.2}CoO_{3-\delta}$ (figure 1(a)) and $ACo_{0.8}Bi_{0.2}O_{3-\delta}$ (figure 1(b)) samples were single-phase and cubic in structure. The results indicate that the Bi ions had been incorporated into the perovskite lattice. The used $ACo_{0.8}Bi_{0.2}O_{3-\delta}$ catalyst showed no significant change in XRD features (figure 1(c)). After the TPR experiment, the XRD pattern of the Bi-doped catalyst (figure 1(d)) changed considerably and new phases such as

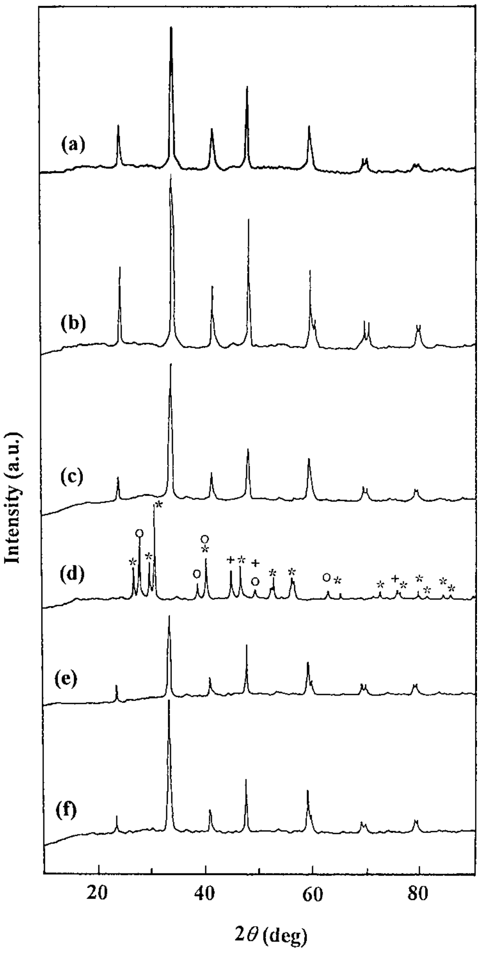

Figure 1. XRD patterns of (a) fresh $La_{0.8}Ba_{0.2}CoO_{3-\delta}$ and (b–f) $ACo_{0.8}Bi_{0.2}O_{3-\delta}$: (b) fresh sample, (c) after CO oxidation reaction, (d) after TPR, (e) after reoxidation of the TPR sample in O_2 (20 ml min^{-1}) at 800 °C for 1 h, and (f) after 100 pulses of CO at 450 °C. Symbol "∗" denotes the La_2O_3 phase, "O" the Bi^0 phase, and "+" the Co^0 phase.

La_2O_3, metallic Co^0, and metallic Bi^0 were formed, indicating that the $ACo_{0.8}Bi_{0.2}O_{3-\delta}$ sample was reduced (by H_2) and the perovskite structure was destroyed. However, upon the reoxidation of the reduced $ACo_{0.8}Bi_{0.2}O_{3-\delta}$ sample (figure 1(e)), the signals corresponding to a single-phase cubic perovskite structure reappeared with a slight decrease in line intensity. The similarity between figure 1 (f) and (b) suggests that the $ACo_{0.8}Bi_{0.2}O_{3-\delta}$ sample was rather intact in 100 pulses of CO at 450 °C. According to the results of chemical analysis, there were 56.1 mol% Co^{2+}, 43.9 mol% Co^{3+}, 99.2 mol% Bi^{5+}, and 0.8 mol% Bi^{3+} in fresh $ACo_{0.8}Bi_{0.2}O_{3-\delta}$; and 8.3 mol% Co^{4+} and 91.7 mol% Co^{3+} in fresh $La_{0.8}Ba_{0.2}CoO_{3-\delta}$. Considering the titration uncertainty, one can take that the Bi ions were practically pentavalent. According to the principle of electroneutrality, the δ values were estimated to be 0.13 for $ACo_{0.8}Bi_{0.2}O_{3-\delta}$ and 0.06 for $La_{0.8}Ba_{0.2}CoO_{3-\delta}$. The BET specific surface areas of the undoped and Bi-doped catalysts were 6.1 and 5.6 $m^2\,g^{-1}$, respectively.

Figure 2 shows the catalytic activities of $ACo_{0.8}Bi_{0.2}O_{2.87}$ versus reaction temperature at 30000 h^{-1} and at three different CO/O_2 molar ratios. For comparison purposes, the activity of $La_{0.8}Ba_{0.2}CoO_{2.94}$ as related to temperature at $CO/O_2 = 0.67/1.00$ is also included. It is observed that over the Bi-free catalyst and with the rise in reaction temperature, CO conversion increased; at 330 °C, 100% CO conversion was reached. Over the Bi-incorporated catalyst in the three reaction atmospheres, CO conversion increased markedly with temperature rise; 100% CO conversion was achieved at 250 °C for $CO/O_2 = 0.67/1.00$, at 290 °C for $CO/O_2 = 1.75/1.00$, and at 310 °C for $CO/O_2 = 2.01/1.00$. Apparently, the temperature required for complete CO conversion increased with a drop in O_2 content. Compared to the catalysts of supported noble metals (Pt, Pd or Rh), the catalysts of base metal oxides usually exhibit a significant drawback, i.e., there is a rapid decrease in CO conversion at elevated space velocities [3]. In order to examine this effect over $ACo_{0.8}Bi_{0.2}O_{2.87}$, we tested the catalyst at various space velocities and the results are shown in figure 3. With the increase in space velocity from 5000 to 60000 h^{-1}, the

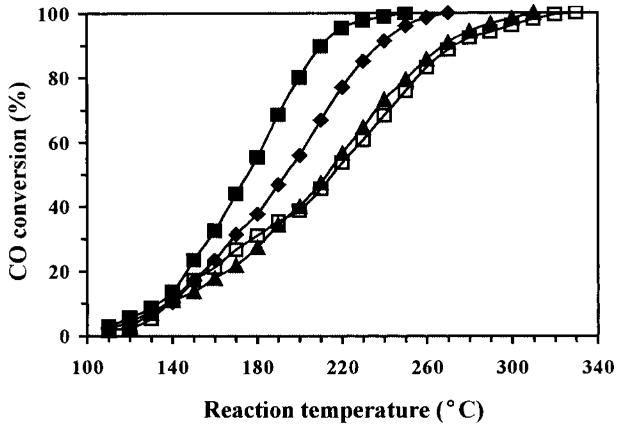

Figure 2. Catalytic performance of $La_{0.8}Ba_{0.2}CoO_{2.94}$ (□) and $ACo_{0.8}Bi_{0.2}O_{2.87}$ (■, ◆, ▲) as related to reaction temperature at space velocity 30000 h^{-1} and CO/O_2 molar ratios 0.67/1.00 (□, ■), 1.75/1.00 (◆), and 2.01/1.00 (▲).

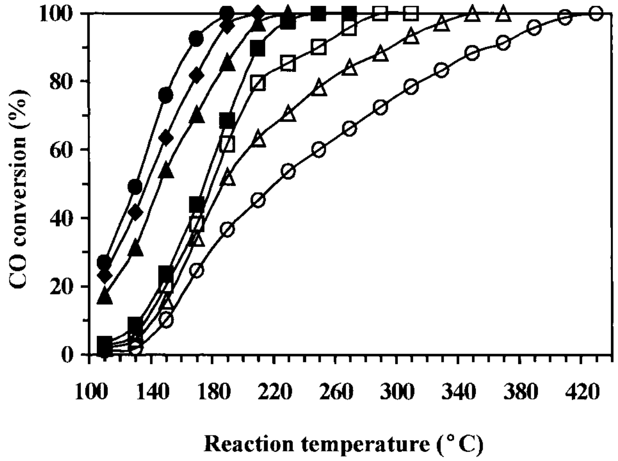

Figure 3. Catalytic performance of $ACo_{0.8}Bi_{0.2}O_{2.87}$ as a function of reaction temperature at CO/O_2 molar ratio 0.67/1.00 and space velocities 5000 (•), 10000 (◆), 20000 (▲), 30000 (■), 40000 (□), 50000 (△), and 60000 h^{-1} (○).

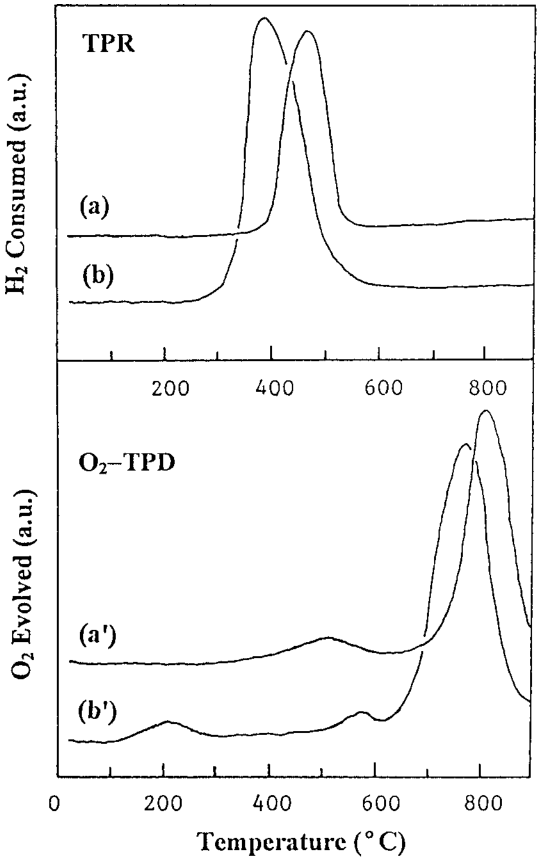

Figure 4. TPR and O_2-TPD profiles of $La_{0.8}Ba_{0.2}CoO_{2.94}$ (a, a′) and $ACo_{0.8}Bi_{0.2}O_{2.87}$ (b, b′).

temperature for 100% CO conversion shifted from 190 to 430 °C. Furthermore, CO conversions augmented at a much faster rate at lower space velocities. We observed similar scenarios in the $CO/O_2 = 1.75/1.00$ and 2.01/1.00 cases.

3.2. TPR and O_2-TPD studies

Figure 4 illustrates the TPR and O_2-TPD profiles of $La_{0.8}Ba_{0.2}CoO_{2.94}$ and $ACo_{0.8}Bi_{0.2}O_{2.87}$. There was a big reduction band at ca. 490 °C for the former sample (figure 4(a)) and at ca. 400 °C for the latter sample (figure 4(b)); both were due to catalyst reduction as corroborated by the XRD results (figure 1(d)). For the O_2-TPD profile of the Bi-free catalyst (figure 4(a′)), a small desorption peak at ca. 510 °C and a large one at ca. 806 °C were observed; the corresponding amounts of O_2 desorption were 4.8 and 70.2 $\mu\mathrm{mol\,g_{cat}^{-1}}$. As for the O_2-TPD profile of the Bi-doped catalyst (figure 4(b′)), there were desorption peaks at ca. 205 and 565 °C (both are small and broad) and a large one at ca. 768 °C; the amounts of O_2 desorption were 8.8 $\mu\mathrm{mol\,g_{cat}^{-1}}$ for the first two peaks and 90.6 $\mu\mathrm{mol\,g_{cat}^{-1}}$ for the last one.

3.3. $^{18}O_2$- and CO-pulsing studies

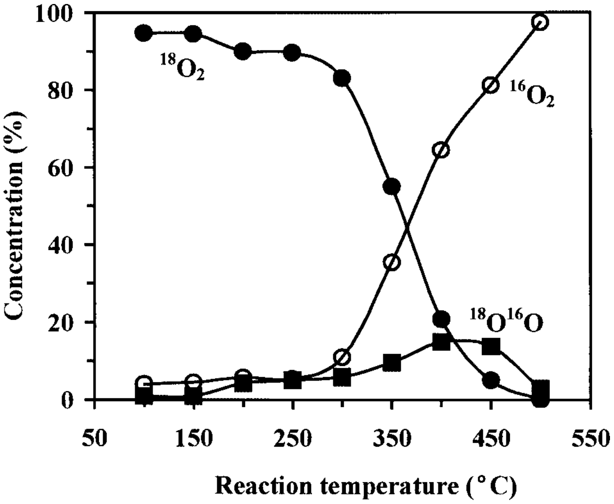

Figure 5. The distribution of isotopic dioxygen in the $^{18}O/^{16}O$ exchange experiment performed over $ACo_{0.8}Bi_{0.2}O_{2.87}$ (after treatment in He at 700 °C for 30 min) at various temperatures.

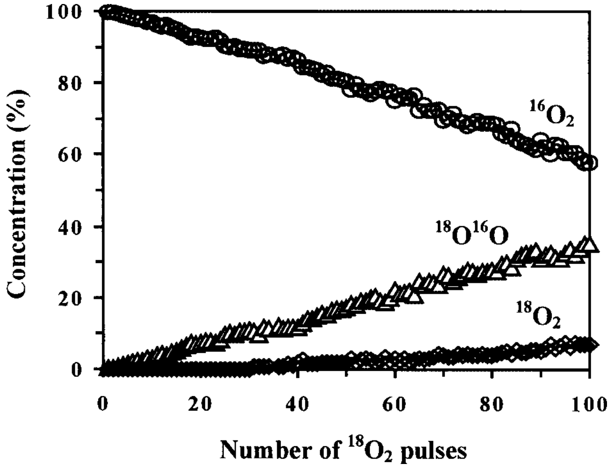

Figure 6. The variation of $^{16}O_2$, $^{18}O^{16}O$, and $^{18}O_2$ concentrations as related to pulse number during $^{18}O_2$ pulsing at 500 °C over an $ACo_{0.8}Bi_{0.2}O_{2.87}$ sample which had been treated in He at 700 °C for 30 min.

Figure 5 shows the distribution of dioxygen in the pulsing of $^{18}O_2$ onto the $ACo_{0.8}Bi_{0.2}O_{2.87}$ catalyst at different temperatures. When the temperature was raised to 200 °C, isotopic exchange (between the ^{18}O from the gas phase and the ^{16}O in the catalyst lattice) took place. Above 300 °C, the exchange became significant. At 425 °C, the concentration of $^{18}O^{16}O$ was the highest. Further rise in temperature toward 500 °C resulted in a decrease in $^{18}O^{16}O$ and a considerable increase in $^{16}O_2$ concentration; at 500 °C, the exchange came to a completion. The results clearly depict that (i) the lattice oxygen of $ACo_{0.8}Bi_{0.2}O_{2.87}$ became mobile above 300 °C and (ii) the lattice of the catalyst could be readily replenished with gas-phase oxygen.

To further examine the mobility of the lattice oxygen in $ACo_{0.8}Bi_{0.2}O_{2.87}$, we kept on pulsing $^{18}O_2$ at 500 °C onto the catalyst and the results of up to 100 pulses are shown in figure 6. With the increase in pulse number, $^{16}O_2$ concentration decreased, whereas $^{16}O^{18}O$ and $^{18}O_2$ concentrations increased with the former augmenting much faster than the

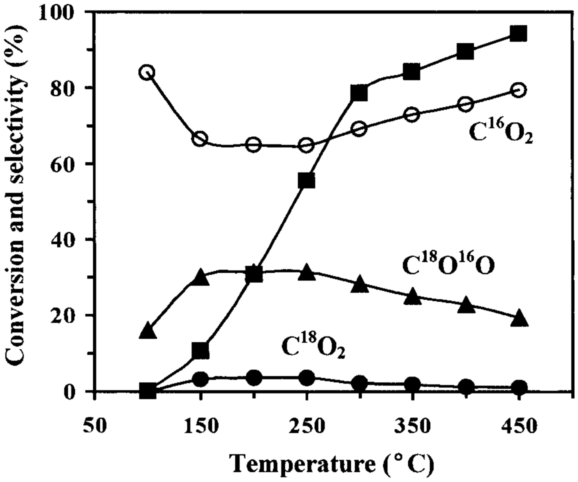

Figure 7. CO conversion (■) and the distribution of isotopic carbon dioxide at the 10th pulse of CO over $ACo_{0.8}Bi_{0.2}O_{2.87}$ (after treatment in He at 700 °C for 30 min and 100 pulses of $^{18}O_2$ at 500 °C) at various temperatures.

latter. During the pulsing of $^{18}O_2$, ^{18}O infiltrated into the lattice, driving $^{16}O_2$ and $^{18}O^{16}O$ into the gas phase. The slow increase in $^{18}O_2$ content and the rapid rise in $^{18}O^{16}O$ concentration demonstrate that ^{18}O could diffuse easily into the catalyst, implying that mobility of lattice oxygen in $ACo_{0.8}Bi_{0.2}O_{2.87}$ was rather high at 450 °C. The continuous drop in $^{16}O_2$ content is an indication of ^{16}O deprivation after prolonged replacement by ^{18}O.

In order to investigate the reactivity of lattice oxygen species, we pulsed CO at various temperatures onto an $ACo_{0.8}Bi_{0.2}O_{2.87}$ sample that had been treated in He at 700 °C for 30 min and exposed to 100 pulses of $^{18}O_2$ at 500 °C; the data were obtained at the 10th pulse of CO (figure 7). With temperature rise, there was a general increase in CO conversion. Between 150 and 250 °C, the selectivity of $C^{16}O_2$ was ca. 75% while that of $C^{18}O^{16}O$ was ca. 30%; the selectivity of $C^{18}O_2$ was below 3%. The balance of carbon was found to be within the range of 99.5–100% throughout the whole temperature range.

4. Discussion

4.1. Defect structure and catalytic activity

Among the A-substituted $LaCoO_3$ series, Sr-substitution for La has been studied most extensively and intensively [3]. Due to the similarity in chemical properties, Ba-substitution for La is expected to induce effects similar to Sr-substitution for La: the generation of oxygen vacancies and hypervalent cobalt ions (Co^{4+}). The positive value of δ ($= 0.06$) and the presence of 8.3 mol% Co^{4+} ions in $La_{0.8}Ba_{0.2}CoO_{3-\delta}$ confirmed such a deduction. The ionic radii of Co^{3+} (0.55 Å, coordination number (CN) = 6) and Co^{2+} (0.65 Å, CN = 6) are smaller than that of Bi^{5+} (0.76 Å, CN = 6), whereas the size of Bi^{3+} (1.03 Å, CN = 6; 1.17 Å, CN = 8, no information for CN = 12 is available in the literature) is smaller than those of La^{3+} (1.36 Å, CN = 12) and Ba^{2+} (1.61 Å, CN = 12) [36]. According to the estimation of tolerance factor [3], Bi^{3+} should dwell at the A sites while Bi^{5+} at the B sites of ABO_3. Such a notion has been substantiated by Khasanova et al. [37,38] who investigated the crystal structures of $K_{1-x}Bi_xBiO_{3-\delta}$, and by Zanne et al. [39] and Boullay et al. [40] who studied the structures of Ba–Bi–Fe–O perovskites. It is unusual to have both A and B sites occupied by the same element. The result of chemical analysis for Bi oxidation state indicated that the Bi ions in $ACo_{0.8}Bi_{0.2}O_{2.87}$ were pentavalent. Since Bi^{5+} is bigger than Co^{2+} and Co^{3+}, the incorporation of Bi^{5+} ions into the B sites would enlarge the $La_{0.8}Ba_{0.2}CoO_{3-\delta}$ lattice. With $ACo_{0.8}Bi_{0.2}O_{2.87}$ being supposed to fit a cubic symmetry, we used the least squares refinement method to calculate the lattice parameters (according to the d values of the XRD pattern of the fresh sample); the lattice parameter (a) was estimated to be 5.5902 Å, considerably larger than that (5.4796 Å) of $La_{0.8}Ba_{0.2}CoO_3$. With the expansion (ca. 2%) of the lattice, there should be weakening of the Co–O and Bi–O bonds, and the result is the enhancement in lattice oxygen mobility. Furthermore, the amount (δ) of oxygen nonstoichiometry in $ACo_{0.8}Bi_{0.2}O_{3-\delta}$ was 0.13, indicating that there was a substantial amount of oxygen vacancies. The enhancement in lattice oxygen mobility (as depicted in the results of TPR, $^{18}O/^{16}O$ isotopic exchange, and CO-pulsing studies) and the presence of oxygen vacancies rendered the nonstoichiometric perovskite material catalytically active for CO oxidation.

In the steady-state oxidation of CO over supported metal catalysts, there is a critical CO/O_2 molar ratio at which the rate-determining step shifts from CO adsorption to O_2 dissociation [41–46]. Below this critical ratio, the amount of adsorbed oxygen is higher than that of adsorbed CO; at high CO concentrations, the surface would be lack of adsorbed oxygen. Over perovskite catalysts, O_2 could be activated readily at structural defects. Compared to O_2 activation, the activation of CO over perovskites is difficult. Working on a $LaCoO_{3-\delta}$ catalyst by means of FT-IR, Tejuca and co-workers [47–49] concluded that CO adsorbs either on the oxygen atoms adjacent to Co atoms, forming carbonate adspecies or on the Co atoms adjacent to oxygen vacancy, producing carbonyl adspecies. Earlier, we detected both carbonyl and carbonate adspecies after CO adsorption on $La_{0.6}Sr_{0.4}Co_{1-x}M_xO_3$ [50]. Similar species are expected to be detected on $ACo_{0.8}Bi_{0.2}O_{2.87}$. The decrease in surface oxygen concentration undermines the process of lattice oxygen replenishment. As shown in figure 2, the temperature required for 100% conversion of CO to CO_2 increased with the drop in O_2 content. Therefore, it is understandable that in an O_2-rich atmosphere, CO oxidation could proceed at a relative lower temperature. Unlike those observed over precious metal catalysts, the catalytic activities of perovskites for CO oxidation are more sensitive to the change in space velocity. In an O_2-rich atmosphere (CO/O_2 molar ratio = 0.67/1.00), the temperature for 100% CO conversion rose with the rise in space velocity (figure 3). Apparently, the

$ACo_{0.8}Bi_{0.2}O_{2.87}$ catalyst showed good performance for CO oxidation under oxidizing conditions.

It is generally believed that CO oxidation proceeds via the interaction of adsorbed CO with adsorbed [51,52] and lattice oxygen [53–57]. The former is oxygen adsorbed dissociatively at oxygen vacancies, usually called α oxygen in O_2-TPD studies [58–61]. This kind of oxygen species is generally believed to be responsible for the total oxidation of CO and HC. The latter is generally called β oxygen in O_2-TPD studies and can be related to the partial reduction of B-site cation [60,61]. Apparently, the α oxygen of $La_{0.8}Ba_{0.2}CoO_{2.94}$ and $ACo_{0.8}Bi_{0.2}O_{2.87}$ enhances the conversion of CO. It has been reported that the redox reactions of cobalt ions with lattice oxygen in $La_{1-x}A'_xBO_{3-\delta}$ ($A' = Ca, Sr$; $B = Mn, Fe, Co$) have an important role to play in enhancing ammoxidation activity [8]. We suggest that the catalytic activities of $La_{0.8}Ba_{0.2}CoO_{2.94}$ and $ACo_{0.8}Bi_{0.2}O_{2.87}$ could be attributed to the extent of the redox processes:

$$2Co^{4+} + O^{2-}_{lattice} \rightleftharpoons 2Co^{3+} + (1/2)O_2 \tag{2}$$

$$2Co^{3+} + O^{2-}_{lattice} \rightleftharpoons 2Co^{2+} + (1/2)O_2 \tag{3}$$

$$Co^{2+} + O^{2-}_{lattice} \rightleftharpoons Co^{0} + (1/2)O_2 \tag{4}$$

$$Bi^{5+} + O^{2-}_{lattice} \rightleftharpoons Bi^{3+} + (1/2)O_2 \tag{5}$$

$$2Bi^{3+} + 3O^{2-}_{lattice} \rightleftharpoons 2Bi^{0} + (3/2)O_2 \tag{6}$$

As illustrated in the O_2-TPD studies (figure 4 (a′) and (b′)), the extent of α oxygen desorption (below 600 °C) over $ACo_{0.8}Bi_{0.2}O_{2.87}$ (8.8 $\mu mol\, g_{cat}^{-1}$) was larger than that over $La_{0.8}Ba_{0.2}CoO_{2.94}$ (4.8 $\mu mol\, g_{cat}^{-1}$), indicating that the amount of oxygen vacancies in the former was higher than that in the latter. The amount of β oxygen desorption over $ACo_{0.8}Bi_{0.2}O_{2.87}$ (90.6 $\mu mol\, g_{cat}^{-1}$) was significantly larger than that over $La_{0.8}Ba_{0.2}CoO_{2.94}$ (70.2 $\mu mol\, g_{cat}^{-1}$), indicating that the incorporation of Bi^{5+} into the $La_{0.8}Ba_{0.2}CoO_{3-\delta}$ lattice promoted the mobility of lattice oxygen. Furthermore, the reduction temperature of $ACo_{0.8}Bi_{0.2}O_{2.87}$ (figure 4(b)) was much lower than that of $La_{0.8}Ba_{0.2}CoO_{2.94}$ (figure 4(a)), meaning that the mobility of lattice oxygen in the former catalyst was higher than that in the latter catalyst. Therefore, the enhanced catalytic activity of $ACo_{0.8}Bi_{0.2}O_{2.87}$ could be associated with the promotion in lattice oxygen mobility.

4.2. Lattice oxygen mobility

After investigating the reactivity of lattice oxygen and the desorption of oxygen over cobaltate perovskites, Nakamura et al. [62] pointed out (i) the involvement of lattice oxygen, (ii) the reduction of Co^{4+} to Co^{3+}, and (iii) the formation of oxygen vacancies in the CO oxidation reaction. Naturally, with the generation of surface vacancies, the diffusion of lattice oxygen from the bulk to the surface would become facile and the surface oxygen consumed in the reaction could be replenished. Compared to $LaCoO_{3-\delta}$ (O_2 desorption 29.4 $\mu mol\, g_{cat}^{-1}$ at ca. 820 °C [63]), $La_{0.8}Sr_{0.2}CoO_{3-\delta}$ (72.0 $\mu mol\, g_{cat}^{-1}$ at ca. 815 °C [63]), and $La_{0.8}Ba_{0.2}CoO_{3-\delta}$ (70.2 $\mu mol\, g_{cat}^{-1}$ at ca. 806 °C), the $ACo_{0.8}Bi_{0.2}O_{2.87}$ material showed a larger amount (90.6 $\mu mol\, g_{cat}^{-1}$) of β (lattice oxygen) desorption at a lower temperature (ca. 768 °C, figure 4(b′)). The desorption of lattice oxygen induced the partial reductions of Co^{3+} to Co^{2+} (or Co^0) and Bi^{5+} to Bi^{3+} (or Bi^0) via the steps (3)–(6).

The feasibility of bulk reduction (by H_2) at ca. 400 °C (figure 4(b′)) is indicative of the high mobility of the lattice oxygen in $ACo_{0.8}Bi_{0.2}O_{2.87}$. This is confirmed by the results of $^{18}O/^{16}O$ exchange (figure 5) and CO-pulsing (figure 7) studies. Generally speaking, the isotopic exchange involves six different steps [64]:

$$^{18}O_2(g) + {}^{16}O(*) \rightarrow {}^{18}O^{16}O(g) + {}^{18}O(*) \tag{7}$$

$$^{18}O^{16}O(g) + {}^{16}O(*) \rightarrow {}^{16}O_2(g) + {}^{18}O(*) \tag{8}$$

$$^{18}O_2(g) + 2{}^{16}O(*) \rightarrow {}^{16}O_2(g) + 2{}^{18}O(*) \tag{9}$$

$$^{18}O^{16}O(g) + 2{}^{16}O(*) \rightarrow {}^{16}O_2(g) + {}^{18}O(*) + {}^{16}O(*) \tag{10}$$

$$^{18}O_2(g) + {}^{16}O_2(g) \rightarrow 2{}^{18}O^{16}O(g) \tag{11}$$

$$^{18}O^{16}O(g) + 2{}^{18}O(*) \rightarrow {}^{18}O_2(g) + {}^{18}O(*) + {}^{16}O(*) \tag{12}$$

where (g) denotes gas phase and (∗) adsorbed or lattice oxygen. Since the catalyst had been purged with He at 700 °C for 30 min before the pulsing of $^{18}O_2$ (this treatment would guarantee the desorption of the adsorbed oxygen species, as illustrated in the O_2-TPD study (figure 4(b′)), one can preclude the existence of adsorbed ^{16}O species on the surface or at the oxygen vacancies of the catalyst; i.e., the ^{16}O atoms in the desorbed $^{18}O^{16}O$ and $^{16}O_2$ were entirely originated from the lattice oxygen of the catalyst. By comparing the relative concentrations of $^{18}O_2$, $^{18}O^{16}O$, and $^{16}O_2$, one can deduce that below 300 °C, the $^{18}O/^{16}O$ exchange processes proceeded mainly via steps (7)–(12); between 300 and 450 °C, via steps (7)–(11); and at 500 °C, via steps (7)–(10).

The facile infiltration of ^{18}O into the perovskite lattice and the rapid replenishment of the consumed amount of lattice oxygen by gas-phase oxygen demonstrate the high mobility of lattice oxygen in $ACo_{0.8}Bi_{0.2}O_{2.87}$. Other supporting evidence is from the results of $^{18}O_2$ pulsing at 500 °C (figure 6): with the increase in pulse number, there is a sharp rise in $^{18}O^{16}O$ concentration and a continuous drop in $^{16}O_2$ (originated from the catalyst) population, indicating that the exchange process between ^{18}O (from the gas phase) and ^{16}O (in the catalyst) is facile. In other words, the lattice oxygen of $ACo_{0.8}Bi_{0.2}O_{2.87}$ is rather mobile. As shown in figure 7, the high $C^{18}O^{16}O$ selectivity in the range of 150–250 °C and the high CO conversion in the range of 250–450 °C reflect the high reactivity of lattice $^{18}O^{2-}$ (incorporated into in the catalyst during $^{18}O_2$ pulsing) with CO; i.e., the lattice oxygen is reactive toward CO. It should be noted that the near 100% carbon balance at or below 450 °C precludes the possibility of CO disproportionation ($2CO \rightarrow C + CO_2$). Previously, we have reported that CO disproportionation occurred only above 460 °C over a $Ni–La_2O_3/5A$ catalyst [65]. This Ni-based catalyst is expected to catalyze CO disproportionation reaction more readily than a perovskite-type oxide catalyst such as $ACo_{0.8}Bi_{0.2}O_{2.87}$ because metallic nickel can activate CO molecules more effectively than the base metal oxides. Based on these results and the above consideration, we deduce that the lattice oxygen in $ACo_{0.8}Bi_{0.2}O_{2.87}$ is responsible for the low-temperature catalytic reaction of CO oxidation.

5. Conclusions

The $La_{0.8}Ba_{0.2}CoO_{2.94}$ and $ACo_{0.8}Bi_{0.2}O_{2.87}$ ($A = La_{0.8}Ba_{0.2}$) catalysts were single phase and cubic in structure; there were Co^{4+} and Co^{3+} ions in the former and Co^{3+}, Co^{2+}, and Bi^{5+} ions in the latter. The Bi-incorporated catalyst performed better than the Bi-free catalyst. Over $ACo_{0.8}Bi_{0.2}O_{2.87}$ at a same space velocity, the temperature for 100% CO conversion became higher with a rise in CO/O_2 molar ratio, whereas with a drop in space velocity at an equal CO/O_2 molar ratio, it became lower. The best activity (100% CO conversion at 190 °C) of the Bi-doped catalyst was at a space velocity of 5000 h^{-1} and a CO/O_2 molar ratio of 0.67/1.00. The O_2-TPD investigation revealed that the presence of Bi^{5+} ions caused the desorption temperature of lattice oxygen to decrease. The results of TPR, $^{18}O/^{16}O$ isotopic exchange, and CO-pulsing investigations confirmed that the lattice oxygen in the catalyst is highly mobile. Based on these results, we conclude that (i) the catalytic performance of the Bi-incorporated perovskite material could be associated with structural defects, and (ii) the high mobility of lattice oxygen is responsible for the activity of low-temperature CO oxidation.

Acknowledgement

The work described in this paper was fully supported by a grant from the Hong Kong Baptist University (FRG/00-01/I-15).

References

[1] R.J.H. Voorhoeve, D.W. Johnson, Jr., J.P. Remeika and P.K. Gallagher, Science 195 (1977) 827.

[2] R.E. Newman, in: *Structure–Property Relationship in Perovskite Electroceramics: Perovskite: A Structure of Great Interest to Geophysics and Material Science*, eds. A. Navrotsky and D.J. Weidner (Am. Geophys. Union, Washington, DC, 1989).

[3] L.G. Tejuca and J.L.G. Fierro, eds., *Properties and Applications of Perovskite-Type Oxides* (Dekker, New York, 1993).

[4] M.L. Rojas, J.L.G. Fierro, L.G. Tejuca and A.T. Bell, J. Catal. 124 (1990) 41.

[5] H. Yasuda, Y. Fujiwara, N. Mizuno and M. Misono, J. Chem. Soc. Faraday Trans. 90 (1994) 1183.

[6] L. Lisi, G. Bagnasco, P. Ciambelli, S. De Rossi, P. Porta, G. Russo and M. Turco, J. Solid State Chem. 146 (1999) 176.

[7] K. Tabata, Y. Hirano and E. Suzuki, Appl. Catal. A 170 (1998) 245.

[8] Y. Wu, T. Yu, B.S. Dou, C.X. Wang, X.F. Xie, Z.L. Yu, S.R. Fan, Z.R. Fan and L.C. Wang, J. Catal. 120 (1989) 88.

[9] K.R. Barnard, K. Foger, T.W. Turney and R.D. Williams, J. Catal. 125 (1990) 265.

[10] T. Nitadori, S. Kurihara and M. Misono, J. Catal. 98 (1986) 221.

[11] S. Rajadurai, J.J. Carberry, B. Li and C.B. Alcock, J. Catal. 131 (1991) 582.

[12] R. Doshi, C.B. Alcock and J.J. Carberry, Catal. Lett. 18 (1993) 337.

[13] K.S. Song, H.X. Cui, S.D. Kim and S.K. Kang, Catal. Today 47 (1999) 155.

[14] S. Ramesh and M.S. Hegde, J. Phys. Chem. 100 (1996) 8443.

[15] Y. Xuan, C.H. He, R. Wang, R. Liu and Y.Q. Jia, Catal. Lett. 46 (1997) 119.

[16] W. Li, H.X. Dai and Y.W. Liu, Stud. Surf. Sci. Catal. 75 (1992) 1793.

[17] W. Li, in: *Properties and Applications of Perovskite-Type Oxides*, eds. L.G. Tejuca and J.L.G. Fierro (Dekker, New York, 1993) p. 145.

[18] J. Mizusaki, Y. Mima, S. Yamamuchi and K. Fueki, J. Solid State Chem. 80 (1989) 102.

[19] A.N. Petrov, V.A. Cherepanov, O.F. Kononchuk and L.Ya. Gavrilova, J. Solid State Chem. 87 (1990) 69.

[20] J. Mizusaki, Solid State Ionics 52 (1992) 79.

[21] A.N. Petrov, O.F. Kononchuk, A.V. Andreev, V.A. Cherepanov and P. Kofstad, Solid State Ionics 80 (1995) 189.

[22] L.T. Weng, S.Y. Ma, P. Ruiz and B. Delmon, J. Mol. Catal. 11 (1992) 455.

[23] D. Dissanayake, K.C.C. Kharas, J.H. Lunsford and M.P. Rosynek, J. Catal. 139 (1993) 652.

[24] Y. Inoue, H. Sano and Z. Sato, J. Mater. Sci. Lett. 8 (1989) 17.

[25] W. Ueda, S.W. Lin and I. Tohmoto, Catal. Lett. 44 (1996) 241.

[26] L. Moens, P. Ruiz, B. Delmon and M. Devillers, Catal. Lett. 46 (1997) 93.

[27] R.J. Cava, B. Batlogg, J.J. Krajeweski, R.C. Farrow, L.W. Rupp, Jr., A.E. White, K.T. Peck, Jr. and T.Y. Kometani, Nature 332 (1988) 814.

[28] D.G. Hinks, B. Dabrowski, J.D. Jorgensen, A.W. Mitchell, D.R. Richards, S. Pei and D. Shi, Nature 333 (1988) 836.

[29] N.R. Khasanova, A. Yamamoto, S. Tajima, X.J. Wu and K. Tanabe, Physica C 305 (1998) 275.

[30] N.R. Khasanova, F. Izumi, T. Kamiyama, K. Yoshida, A. Yamamoto and S. Tajima, J. Solid State Chem. 144 (1999) 205.

[31] H. Maeda, Y. Tanaka, M. Fukutomi and T. Asano, Jpn. J. Appl. Phys. 27 (1988) L209.

[32] M.A. Subramanian, C.C. Torardi, J.C. Calabrese, J. Gopalakrishnan, K.J. Morrissey, T.R. Askew, R.B. Flippen, U. Chowdhry and A.W. Sleight, Science 239 (1988) 1015.

[33] P. Lee, Y. Gao, H.S. Sheu, V. Petricek, R. Restori, P. Coppens, A. Darovskikh, J.C. Phillips, A.W. Sleight and M.A. Subramanian, Science 244 (1989) 62.

[34] H.X. Dai, C.F. Ng and C.T. Au, J. Catal. 189 (2000) 52.

[35] M. Oku, J. Kimura, M. Omori and K. Hirokawa, Fresenius Z. Anal. Chem. 335 (1989) 382.

[36] D.R. Lide, ed., *Handbook of Chemistry and Physics* (CRC Press, New York, 1998/1999) pp. 12–14.

[37] N.R. Khasanova, A. Yamamoto, S. Tajima, X.-J. Wu and K. Tanabe, Physica C 305 (1998) 275.

[38] N.R. Khasanova, F. Izumi, T. Kamiyama, K. Yoshida, A. Yamamoto and S. Tajima, J. Solid State Chem. 144 (1999) 205.

[39] M. Zanne, C. Gleitzer and J. Aubry, J. Solid State Chem. 14 (1975) 160.

[40] Ph. Boullay, M. Hervieu, N. Nguyen and B. Raveau, J. Solid State Chem. 147 (1999) 45.

[41] T. Matsushima, C.J. Musset and J.M. White, J. Catal. 41 (1976) 397.

[42] T. Matsushima, D.B. Almy and J.M. White, Surf. Sci. 67 (1977) 89.

[43] T. Matsushima and J.M. White, Surf. Sci. 67 (1977) 122.

[44] A. Golchet and J.M. White, J. Catal. 53 (1978) 266.

[45] T. Matsushima, M. Hashimoto and I. Toyoshima, J. Catal. 58 (1979) 303.

[46] M. Ehsasi, M. Matloch, D. Frank, J.H. Block, K. Christmann, F.S. Rys and W. Hirschwald, J. Chem. Phys. 91 (1989) 4949.

[47] J.M.D. Tascón and L.G. Tejuca, Z. Phys. Chem. NF 121 (1980) 63.

[48] J.M.D. Tascón, J.L.G. Fierro and L.G. Tejuca, Z. Phys. Chem. NF 124 (1981) 249.

[49] L.G. Tejuca, C.H. Rochester and J.L.G. Fierro, J. Chem. Soc. Faraday Trans. I 80 (1984) 1089.

[50] W. Li, Q. Huang, W.J. Zhang, B.X. Lin and G.L. Lu, Stud. Surf. Sci. Catal. 30 (1987) 405.

[51] Y.J. Mergler, A. van Aalst, J. van Delft and B.E. Nieuwenhuys, Appl. Catal. B 10 (1996) 245.

[52] Y.J. Mergler, J. Hoebink and B.E. Nieuwenhuys, J. Catal. 167 (1997) 305.

[53] T. Jin, T. Okuhara, G.J. Mains and J.M. White, J. Phys. Chem. 91 (1987) 3310.

[54] S.H. Oh and C.C. Eickel, J. Catal. 112 (1988) 543.

[55] G.S. Zafiris and R.J. Gorte, J. Catal. 143 (1993) 86.

[56] C. Serre, F. Garin, G. Belot and G. Maire, J. Catal. 141 (1993) 9.

[57] A.K. Tripathi and N.M. Gupta, J. Catal. 153 (1995) 208.

[58] N. Yamazoe, Y. Teraoka and T. Seiyama, Chem. Lett. (1981) 1767.

[59] C.N.R. Rao, in: *Chemistry of Oxide Superconductivity*, ed. C.N.R. Rao (Blackwell, Oxford, 1988).

[60] A. Bielañski and J. Haber, *Oxygen in Catalysis* (Dekker, New York, 1991).

[61] J. Haber, in: *Surface Properties and Catalysis by Non-Metals*, eds. J.P. Bonnelle, B. Delmon and E. Derouane (Reidel, Dordrecht, 1983).

[62] T. Nakamura, M. Misono and Y. Yoneda, Chem. Lett. (1981) 1589.

[63] T. Seiyama, N. Yamazoe and K. Eguchi, Ind. Eng. Chem. Prod. Res. Dev. 24 (1985) 19.

[64] K. Klier, J. Nováková and P. Jíru, J. Catal. 2 (1963) 479.

[65] J.Z. Luo, Z.L. Yu, C.F. Ng and C.T. Au, J. Catal. 194 (2000) 198.